Earth and Planetary Science Letters 388 (2014) 59–70

Contents lists available at ScienceDirect

Earth and Planetary Science Letters

www.elsevier.com/locate/epsl

Direct evidence for organic carbon preservation as clay-organic nanocomposites in a Devonian black shale; from deposition to diagenesis

Martin John Kennedy *, Stefan Carlos Löhr, Samuel Alex Fraser, Elizabeth Teresa Baruch

Sprigg Geobiology Centre, School of Earth and Environmental Sciences, University of Adelaide, Adelaide, 5005, SA, Australia

ARTICLE INFO

Article history:
Received 27 June 2013
Received in revised form 21 November 2013
Accepted 21 November 2013
Available online 18 December 2013
Editor: T.M. Harrison

Keywords:
black shale
organic matter preservation
carbon sequestration
nanocomposite
unconventional reservoir
Woodford Shale

ABSTRACT

The burial of marine sourced organic carbon (OC) in continental margin sediments is most commonly linked to oceanographic regulation of bottom-water oxygenation (anoxia) and/or biological productivity. Here we show an additional influence in the Devonian Woodford Shale, in which OC occurs as nanometer intercalations with specific phyllosilicate minerals (mixed-layer illite/smectite) that we term organo-mineral nanocomposites. High resolution transmission electron microscopic (HRTEM) images provide direct evidence of this nano-scale relationship. While discrete micron-scale organic particles, such as Tasmanites algal cysts, are present in some lamina, a strong relation between total organic carbon (TOC) and mineral surface area (MSA) over a range of 15% TOC indicate that the dominant association of organic carbon is with mineral surfaces and not as discrete pelagic grains, consistent with HRTEM images of nanocomposites. Where periods of oxygenation are indicated by bioturbation, this relationship is modified by a shift to lower OC loading on mineral surfaces and reduced MSA variability likely resulting from biological mixing and homogenization of the sediment, oxidative burn down of OC and/or stripping of OC from minerals in animal guts. The TOC–MSA relationship extends across a range of burial depths and thermal maturities into the oil window and persists through partial illitization. Where illitization occurs, the loss of mineral surface area associated with the collapse of smectite interlayer space results in a systematic increase in TOC:MSA and reorganization of organic carbon and clays into nano-scale aggregates. While the Woodford Shale is representative of black shale deposits commonly thought to record heightened marine productivity and/or anoxia, our results point to the importance of high surface area clay minerals for OC enrichment. Given that the vast majority of these clay minerals are formed in soils before being transported to continental margin settings, their mineralogy and attendant preservative potential is primarily a function of continental climate and provenance making these deposits a sensitive recorder of land as well as oceanographic change.

1. Introduction

The burial of OC in marine sediments is one of the most fundamental biogeochemical processes on Earth and not only influences the temperature and oxygenation of the oceans and atmosphere but also comprises the primary source of hydrocarbons (Arthur and Sageman, 1994; Burdige, 2007; Hedges and Keil, 1995). Greater than 95% of organic carbon (OC) preserved at the surface of the Earth is buried in continental margin sediments, but the final portion of OC finding its way into sediments constitutes only a small fraction (<0.5%) of marine primary production (Burdige, 2007; Hedges and Keil, 1995). However, anomalous concentrations of OC within specific intervals of the geologic record imply that the efficiency of carbon burial is variable, and likely attributable to changing environmental conditions.

The origin of anomalous organic enrichment in the geologic record and implications of these deposits remains controversial. While black shale intervals can be strikingly different from background sediment composition and show abrupt onset consistent with a single dominant control, studies of various examples point to a range of empirical associations suggestive of the interplay of various environmental influences (Arthur and Sageman, 1994). Controls most commonly suggested include low or depleted dissolved oxygen concentrations favourable to OC preservation

Abbreviations: EDS, energy dispersive spectroscopy; EGME, Ethylene Glycol Monoethyl Ether; IC, inorganic carbon; MSA, mineral surface area; OC, organic carbon; OM, organic matter; SEM, scanning electron microscope; TEM, transmission electron microscope/microscopy; TOC, total organic carbon; XRD, X-ray diffraction.

* Corresponding author.
E-mail address: martin.kennedy@adelaide.edu.au (M.J. Kennedy).

http://dx.doi.org/10.1016/j.epsl.2013.11.044
0012-821X

(Demaison and Moore, 1979), productivity-dependent OC flux (Calvert et al., 1992; Pedersen and Calvert, 1990) and concentration of OC in sediments by a reduction in siliciclastic dilution (Tyson, 2001).

A first order association between total organic carbon (TOC) and mineral surface area (MSA) in modern continental margin sediments suggests another potentially important influence not commonly considered in ancient organically enriched shales (Mayer, 1994; Hedges and Keil, 1995). This relation is common to most modern sediments studied to date, irrespective of their depositional environment (Keil et al., 1994a; Mayer, 1994; Ransom et al., 1997; Bergamaschi et al., 1997; Keil and Cowie, 1999), although differences in environmental conditions such as nutrient availability and oxygenation are expressed as higher (high productivity, low-oxygen settings) or lower (long oxygen exposure times, high energy environments) OC loadings per unit surface area (Blair and Aller, 2012). An MSA:TOC correlation has also been demonstrated in ancient examples across a range of redox conditions and TOC values from 1% to 20% (Kennedy et al., 2002; Kennedy and Wagner, 2011). Mineral surface associated preservation of OC has the potential to be significant because detrital clay minerals comprise >60% of continental margin sediments and MSA is controlled by the abundance of some common clay minerals with very high surface area (Chamley, 1989; Hedges and Keil, 1995) such as smectite which has two orders of magnitude greater MSA than quartz silt or carbonate.

The physical or chemical mechanism(s) causing the TOC:MSA correlation is yet to be resolved but is key for understanding the extent and significance of this association. Some hypothesized preservative mechanisms include sorption (Keil et al., 1994a; Keil and Cowie, 1999; Mayer, 1994; Satterberg et al., 2003; Baldock and Skjemstad, 2000), physical sheltering or encapsulation by clay mineral aggregates (Ransom et al., 1997; 1998; Salmon et al., 2000; Bock and Mayer, 2000; Zimmerman et al., 2004) and intercalation within hydrating clay minerals as organo-mineral nanocomposites (Kennedy et al., 2002; Kennedy and Wagner, 2011; Theng et al., 1986; Jia et al., 2002; Chen et al., 2008; Sposito et al., 1999). Key questions that remain include how universal this mechanism of preservation is outside the studied examples, what type of mineral surfaces have preservative properties, how much mineral surface-associated OC preservation is influenced by environmental conditions such as varying productivity and oxygenation and/or diagenetic burial processes such as MSA loss through illitization and OC loss though hydrocarbon generation.

The direct approach to identifying the relationship between mineral and OC is through imaging their association(s), but since they occur at 100 nanometer scales and require the technically challenging sample preparation of nanometer thick ultra-thin sections necessary to reveal crystal to crystal boundaries, most studies have focused on indirect means of characterization (Bock and Mayer, 2000; Keil et al., 1994b; Kennedy and Wagner, 2011; Mayer, 1999).

In contrast to the general idea that OC in marine sediments is comprised of discrete, mostly pelagic, particles (similar to those collected in sediment traps near the sea bed), studies of modern sediments show that >80% of these OC particles are mineralized within the first 30 cm downward from the sea floor (Mayer, 1994), and that >90% of the remaining OC cannot be physically separated from the mineral matrix (Keil et al., 1994a). It is the latter fraction that displays strong correlation with MSA. The mineral-associated fraction degrades at a rate five orders of magnitude slower than the same OC when desorbed from mineral surfaces (Keil et al., 1994a), so that the mineral-associated fraction becomes an increasing proportion of the TOC from the seabed downward (Keil et al., 1994a; Mayer, 1994), representing the most likely fraction to enter the geological record. A strong correlation ($R^2 = 85\%$) between MSA and TOC documented in thermally immature Cretaceous sediments from the western interior seaway of North America (Kennedy et al., 2002) and the Deep Ivorian Basin of the eastern Atlantic (Kennedy and Wagner, 2011) suggests this may indeed be an important mechanism of OC accumulation in the geologic record. Both studies concluded that the relationship extended over MSA values sufficiently high to be diagnostic of smectitic clay minerals, suggesting smectite plays a key role in preservation.

Smectite shows a characteristic order of magnitude greater surface area than any other common sedimentary mineral because the silicate layers of smectite consist of an octahedral sheet sandwiched between two tetrahedral sheets, and these fundamental units stack together to form an interlayer between them (smectite ~750 $M^2\,g^{-1}$, illite <150 $M^2\,g^{-1}$, and kaolinite or quartz silt <30 $M^2\,g^{-1}$). The interlayer is expandable so that interlayer sites are accessible to polar and non-polar organics, ions and water (Theng et al., 1986; Sposito et al., 1999; Jia et al., 2002; Williams et al., 2005; Brigatti et al., 2006; Chen et al., 2008). The preservative effect on OC by smectite has thus been hypothesized to be the result of incorporation of molecular scale organic compounds (derived from the physical or chemical break down of organic particles) in the clay interlayer space where it is protected from microbial degradation (Kennedy et al., 2002; Kennedy and Wagner, 2011). How this relationship might change with thermal maturation and diagenetic transformation of both the organic and mineral phases during burial has not previously been investigated in this context. It has long been known that deep burial of argillaceous sediments results in diagenetic transformation of expandable smectite into non-expandable illite (Hower et al., 1976). Illitization also commonly coincides with the ranges of depth and temperature of formation of oil from kerogen (Abid and Hesse, 2007), and is characterized by tetrahedral Al for Si substitution, dehydration, interlayer collapse, loss of internal surface area, as well as replacement of exchangeable cations in the interlayer by fixed K and/or NH_4^+ (Lindgreen et al., 2000; Dainyak et al., 2006). Although there is evidence that some carbonaceous material can remain within the illite interlayer (Ahn et al., 1999), illitization causes expulsion of most OM previously hosted in the smectite interlayer and may also be associated with polymerization of organic compounds (Williams et al., 2005). The loss of surface area and generation of hydrocarbons will alter the relationship between MSA and TOC if hydrocarbons are lost through migration, or increase the carbon to MSA ratio in the absence of migration.

This study investigates the relationship of MSA to TOC in the Late Devonian (~385 Ma) epeiric sea deposits recorded in the Woodford Shale (Comer, 1991). The Woodford Shale is both an important conventional and unconventional hydrocarbon source rock and broadly representative of a phase of worldwide OC deposition potentially related to significant changes in terrestrial weathering and soil formation associated with the expansion of vascular plants (Klemme and Ulmishek, 1991; Algeo et al., 1998). This study utilizes a two-part strategy to characterize the mode and mechanism of carbon burial and preservation. Initially we establish the typical relationship between TOC and MSA across the Formation using the bulk property parameters of MSA and TOC. We then focus on the mechanisms of that relation by direct imaging of organo-mineral associations at the relevant nanometer scales. While these relations can only be imaged over areas of tens of microns at a time, we argue that our observations are consistent with the MSA and TOC ratios of the bulk samples and can thus be up-scaled and taken as representative of the dominant mode of OC preservation in the Woodford Shale. Samples were collected from three cores at different depths in the basin selected to capture a burial-temperature gradient in order to understand the effects of burial diagenesis and clay illitization on the MSA–TOC relationship.

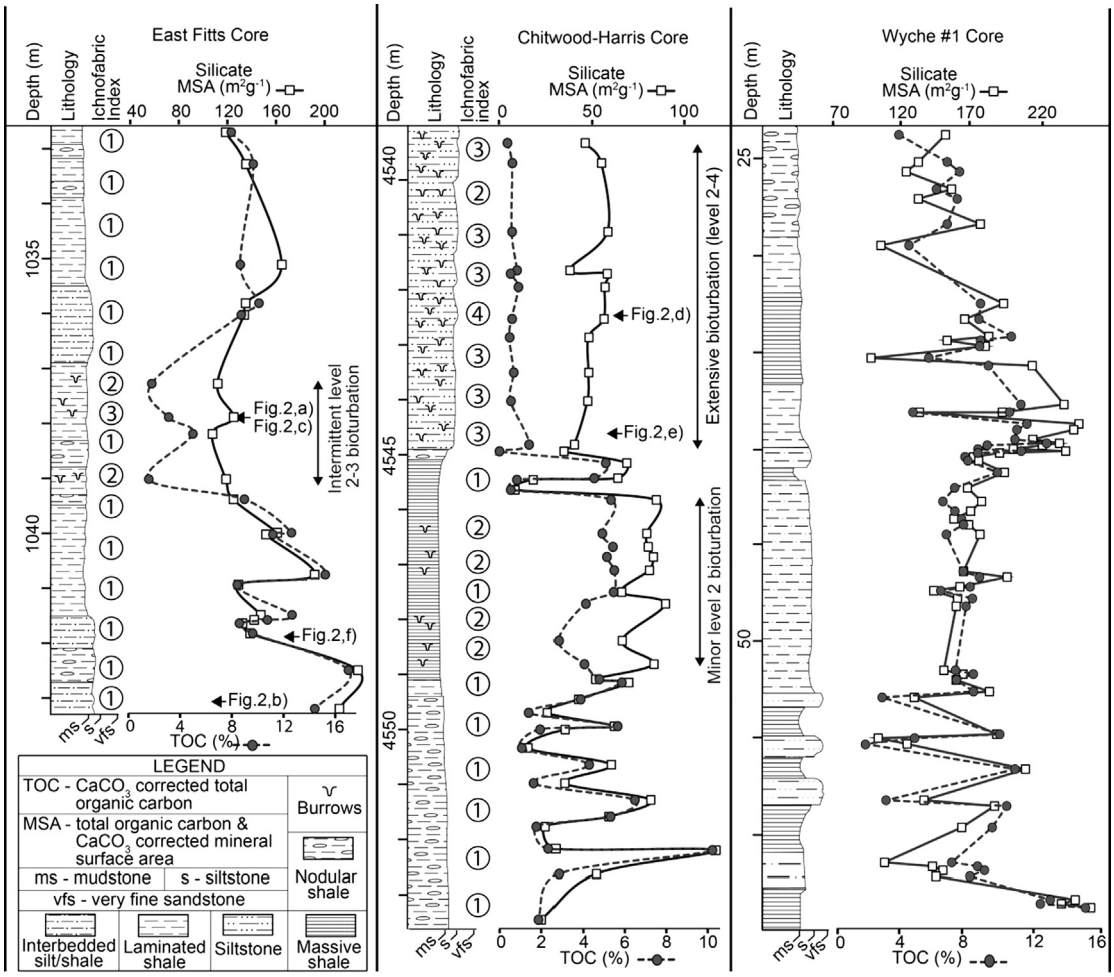

Fig. 1. Lithology, TOC, and silicate MSA, of the East Fitts, Chitwood–Harris and Wyche cores and ichnofabric index (bioturbation intensity) for the East Fitts and Chitwood–Harris core (ichnofabrics were not studied in the Wyche core). Carbonate and OC were subtracted to calculate the MSA of the silicate fraction only to ensure that the patterns observed do not reflect the effects of dilution by components with negligible measurable surface area (see text). Bioturbation intensity was recorded using the Category D Ichnofabric Index of Droser and Bottjer (1993), increasing from level 1 (no bioturbation) to a maximum of level 4 for this study. TOC and MSA vary in phase apart from zones characterized by moderate to high bioturbation which show MSA homogenization and reduction of TOC relative to MSA.

2. The Woodford Shale

The Woodford Shale is an organic rich marine mudstone preserved within a series of basins in modern day Texas, Oklahoma and southeastern New Mexico, USA. The unit reaches burial depths of up to 6000 m (Broadhead, 2010; Comer, 1991; Lo and Cardott, 1995; Miceli Romero and Philp, 2012). OC concentrations in the Woodford Shale typically vary between <1% in siliceous zones to <20% in the black shale facies (Broadhead, 2010; Comer, 1991; Miceli Romero and Philp, 2012). This OC enrichment has been attributed to the combined effects of slow sedimentation and anoxic preservation (Kirkland et al., 1992; Miceli Romero and Philp, 2012). The middle Woodford member, in particular, shows biomarker evidence for continuous water column stratification (gammacerane), bottom-water or pore water anoxia (pristine/phytane ratio) and photic zone euxinia (aryl isoprenoid ratio), with suboxic to dysoxic bottom-water conditions and intermittent photic zone euxinia in lower and upper Woodford members (Miceli Romero and Philp, 2012).

Samples were collected from the Wyche #1 core (Pontotoc County: 34°40.36′N, 96°38.38′W) representing shallow burial at 24 to 65 m (Slatt et al., 2011), the intermediate East Fitts 9-41 core (Pontotoc County: 34°37′16.39″N, 96°33′4.392W) representing intermediate burial at 1033–1043 m, and the Chitwood–Harris-1 core (Grady County: 34°51′05.29″N, 97°49′59.70″W) buried at 4539–4554 m (Fig. 1). Thermal maturity expressed as calculated vitrinite reflectance (%R_o) of the core is as follows: Wyche is immature at 0.38 %R_o, East Fitts is entering the oil window at 0.51 %R_o and Chitwood–Harris core is within the oil window at 0.98 %R_o.

The Woodford Shale core recovery is 41 m thick in the Wyche core, 11 m thick in the East Fitts core and 15 m thick in the Chitwood–Harris core (Fig. 1), and is primarily composed of organic rich shale (Fig. 2f) with intermittent chert intervals (1–10 cm thick) as well as more silty intervals. All sediments lack evidence of storm-wave reworking and are thus considered to have been deposited in relatively deeper, quiet water. Absence of slump structures with only occasional minor indicators of higher energy, preserved as mm scale ripples most likely formed by density currents also suggest a quiet depositional environment. Carbonate content is typically low (<1–5%) with the exception of rare, cm-scale fossiliferous, calcareous zones and calcareous laminated and nodule shale intervals in the Wyche core. Non-calcareous fossils including Tasmanites cysts and radiolaria are present but concentrated in discrete intervals that are widely spaced; they are not recognized throughout the intervals of organic enrichment. Ichnofabrics (trace fossils) record varying degrees of bioturbation in both Chitwood–Harris and East Fitts cores (Fig. 2c to f). The bioturbation index was not determined in the Wyche core and samples represent both bioturbated and unbioturbated intervals.

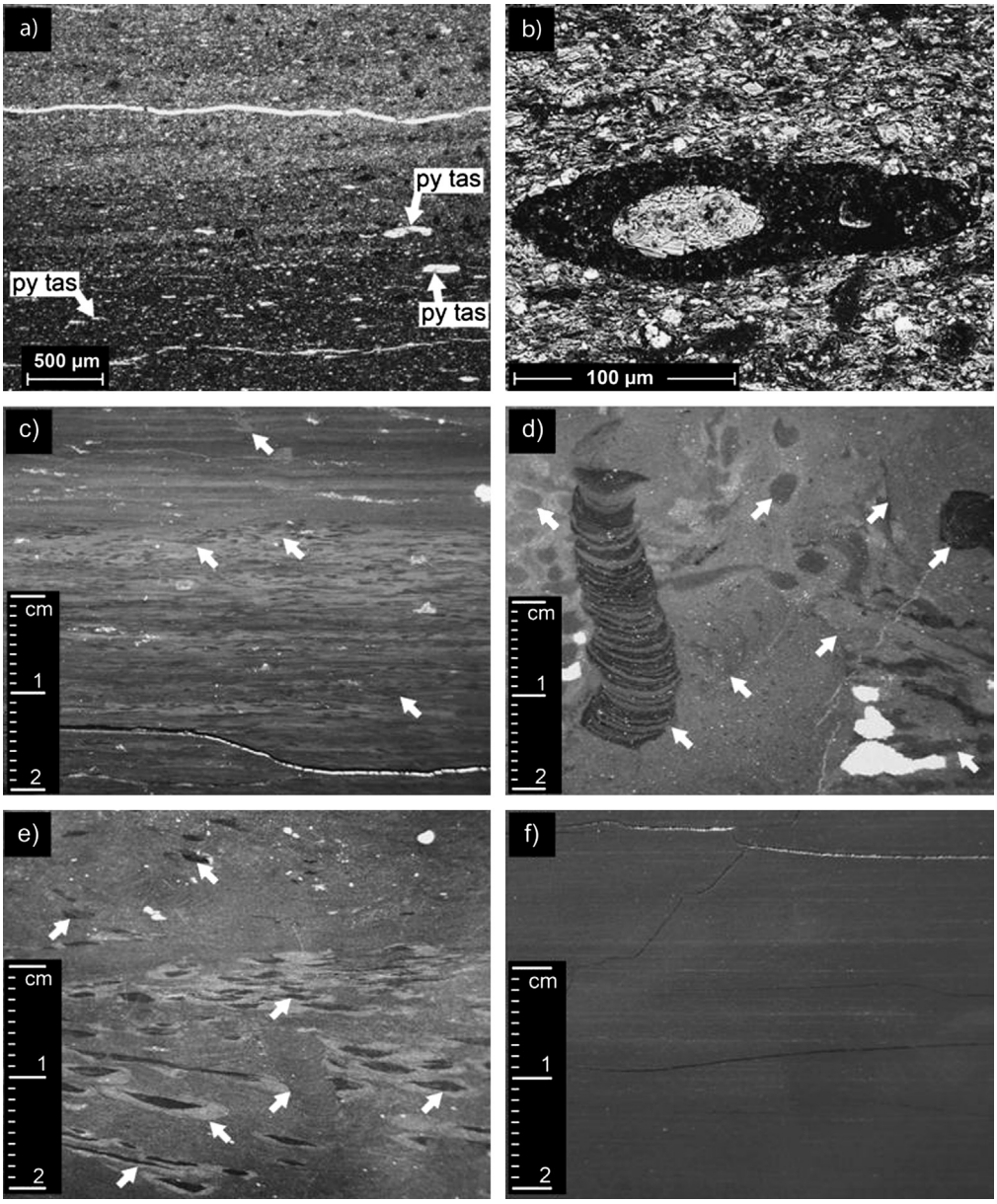

Fig. 2. (a) Photomicrograph (reflected light) of East Fitts (EF) thin section showing laminae of varying composition (quartz or clay dominant). A clay dominant interval hosts pyritized tasmanite fossils (py tas). Tasmanites-rich intervals are generally <1 cm thick, widely spaced and are not present in all samples. Tasmanites are most commonly pyritized and do not contribute to TOC values reported. (b) Backscatter electron SEM image of polished block (EF core), showing a squashed organic-rich tasmanite cyst (dark) with an inorganic core (lighter centre) preserved within a clay-quartz matrix. Discrete, organic particles such as this example are concentrated in narrow bands in the Woodford shale, but their scattered occurrence, frequent pyritization and relatively low abundance mean that they cannot represent the bulk of sediment TOC present in the rock. (c) to (f) are photographs of slab-cut core samples (see Fig. 1 for stratigraphic intervals) showing varying intensities of bioturbation used to identify the ichnofabric index. White arrows mark various examples of trace fossils (burrows). (c) (EF) shows level 2–3 bioturbation featuring overlapping burrows. (d) Chitwood–Harris (CH) example of level 4 bioturbation featuring numerous burrow overlap and extensive laminae disruption. (e) (CH) Example of level 3 bioturbation with overlapping burrows and moderate sediment disruption. (f) Typical sample of unbioturbated sediment (level 1) showing very finely laminated shale with very fine pyritized laminae ($\leqslant$1 mm thick).

3. Methods

A total of 120 sub-samples (59 from Wyche, 20 from East Fitts, and 41 from Chitwood–Harris) selected to capture the MSA and TOC changes with sedimentological and diagenetic variability were milled to a fine powder. MSA was determined using the 'free surface' Ethylene Glycol Monoethyl Ether (EGME) method of Tiller and Smith (1990), and is reported as silicate MSA on an OC and carbonate-free basis to correct for the effects of variable dilution. To determine if EGME was interacting with OM and influencing MSA values, OM was removed from a subset of samples and measured again. These values did not show a drop in MSA values, indicating no effect on MSA of OC (Fig. 7). In contrast to typical MSA measurements using N_2 adsorption (BET), which predominantly measures the external surface area of expandable (smectitic) clay minerals, the EGME method provides a measure of the total surface area (external plus internal; Środoń and McCarty, 2008). This is important in sediments containing an expandable clay component because the protective smectite interlayer surfaces are accessible to a range of organic and inorganic compounds (Johnston, 2010); the total surface area of smectite as measured with EGME is also an order of magnitude greater (approximately 750 $m^2 g^{-1}$) than illite (< 90 $m^2 g^{-1}$) or kaolinite (20 $m^2 g^{-1}$), and almost three orders greater than quartz silt (<10 $m^2 g^{-1}$) or carbonate (<13 $m^2 g^{-1}$) (Kennedy and Wagner, 2011). Thus, where present, even small quantities of smectite can dominate the total sediment mineral

surface area, so that EGME MSAs $>100\ m^2\ g^{-1}$ are a robust indicator for the presence of smectitic clays (Środoń and McCarty, 2008). Comparisons of EGME and BET determined MSA show significant differences in both standard clay materials and Woodford samples (Fig. 7).

East Fitts and Chitwood–Harris samples were measured together, Wyche samples were analyzed as a separate batch. 1 g of each oven-dried (110 °C for 48 h), Ca-exchanged sample was placed in a glass vial, soaked with 1 ml of liquid EGME and placed in a vacuum chamber containing 200 g granular $CaCl_2$ and 40 ml EGME. The air in the chamber was evacuated and samples were allowed to come to equilibrium over approximately 10 days, then weighed every two days until weights stabilized. Samples were weighed for a final time to determine the amount of EGME absorbed, followed by multiplication by a factor of 3.2 to convert this weight (mg) to mineral surface area ($m^2\ g^{-1}$), based on an assumption of monolayer coverage (Tiller and Smith, 1990). Four replicates each of a suite of clay mineral standards obtained from the Clay Mineral Society and included in the same batch as the samples showed good reproducibility (East Fitts + Chitwood–Harris run: SWy-2: 714 $m^2\ g^{-1} \pm 0.7\%$; STx-1b: 729 $m^2\ g^{-1} \pm 2.54\%$; IMt-2: 89 $m^2\ g^{-1} \pm 12.7\%$; Wyche run: SWy-2: 681 $m^2\ g^{-1} \pm 0.81\%$; STx-1b: 695 $m^2\ g^{-1} \pm 1.26\%$; IMt-2: 93 $m^2\ g^{-1} \pm 2.88\%$). Total carbon (TC) content for each sample was measured in a LECO TruMac CN analyzer (for Chitwood–Harris + East Fitts) or a Perkin Elmer 2400 Series II CHNS analyzer (for Wyche). Inorganic carbon (IC, as carbonate) content was determined using the pressure-calcimeter method of Sherrod et al. (2002). OC content was calculated by difference (TC-IC), and is reported on a carbonate-free basis (i.e. corrected for carbonate dilution). BET measurements were made on 0.25 g of powdered sample outgassed under vacuum for 12 h at 110 °C prior to surface area analysis at ~77 K in a MicroMeritics Gemini VII BET surface area analyzer, using N_2 sorption and the 10-point BET (Braun Emmet Teller adsorption isotherm) method.

Thermal maturity of each core was determined by analysis of a subset of samples in a Weatherford Instruments Source Rock Analyzer. Thermal maturity was estimated using the method of Jarvie et al. (2001), which relates measured T_{max} to calculated vitrinite reflectance using the following relationship: calculated $\%R_o = 0.0180 \times T_{max} - 7.16$.

Mineralogy was determined by X-ray diffraction (XRD; Bruker D8 Advance with Cu source) of powdered samples, using Bruker DIFFRAC.EVA software and Crystallography Open Database reference patterns. Clay mineralogy of the samples was determined by XRD using standard methods (Moore and Reynolds, 1997) on oriented preparations of <2 μm separates which were subject to various treatments (air dried, ethylene glycol, heated to 400 and 550 °C). XRD of random powder mounts of the <2 μm fraction of a number of samples was used to determine illite polytypes (Moore and Reynolds, 1997). The <2 μm fraction was obtained by centrifugation after carbonate removal with 1 M sodium acetate buffer at pH 5 and 90 °C, OM removal with NaOCl at pH 9.5 and 90 °C, and ultrasonic dispersal (Lindgreen and Surlyk, 2000). Authigenic quartz was identified using the method of Eslinger et al. (1973), which utilizes the intensity ratio of the I_{100} and I_{101} quartz diffraction peaks on an oriented preparation, where a ratio greater than 0.23 (corresponding to detrital quartz) indicates the presence of authigenic quartz.

The varying intensity of bioturbation in the East Fitts and Chitwood–Harris cores was determined following the category D Ichnofabric Index (Droser and Bottjer, 1993). Light microscope and scanning electron microscope (SEM; FEI Quanta 450 and Philips XL30) imaging of polished blocks and polished thin sections helped determine textural and compositional variability of the Woodford Shale. In addition, nanometer scale associations of clay minerals and OM were assessed using transmission electron microscopy (TEM; Philips CM 200) and energy dispersive spectroscopy (EDS). 80 nanometer thick ultra-thin sections suitable for TEM analysis were prepared following the method of Salmon et al. (2000). The ultra-thin sections were cut perpendicular to the bedding plane from osmium tetroxide (OsO_4) stained, resin-embedded shale subsamples, using a Leica EM UC6 Ultramicrotome equipped with a diamond knife and then transferred onto copper grids with a carbon-free, silicon dioxide support film. Differentiation of OC, resin and void space was based on the recognition of characteristic grey levels for each feature in zones where two or three of these features occur (see also Salmon et al., 2000).

4. Results

The bulk rock samples show a systematic stratigraphic covariance between silicate (carbonate-free fraction) MSA and TOC in all three cores (Fig. 1), where steps of up to 15% TOC are closely matched by proportional shifts in MSA. These cycles show no lead or lag between the two variables. A strong relationship is further demonstrated by the positive linear correlation between TOC and MSA in laminated, undisturbed intervals in all three cores (Fig. 3), with correlation coefficients of $R^2 = 0.94$ (Chitwood–Harris), $R^2 = 0.82$ (East Fitts) and $R^2 = 0.68$ (Wyche). These regressions identify a successively steeper slope with increasing thermal maturity ($\%R_o$) and an x-intercept that steps progressively closer to the origin. Bioturbated intervals (Figs. 1 and 3b) with ichnofabric indices >2 (Fig. 2c to f Chitwood–Harris and East Fitts only), however, show notably less variable MSA and have lower TOC values relative to MSA compared to non-bioturbated intervals. These samples plot off the regression established for undisturbed (laminated) intervals.

Clays, quartz, dolomite, pyrite and feldspar dominate sediment mineralogy. Clay minerals in Chitwood–Harris and East Fitts samples were identified as illite, R3 ordered mixed-layer illite/smectite (<20% smectite) and chlorite (Fig. 4), with chlorite restricted to the more shallowly buried East Fitts samples. Comparison of powder XRD analyses of the <2 μm fraction with diagnostic reflections for illite polytypes (Moore and Reynolds, 1997) show that the illite component in both Chitwood–Harris and East Fitts samples is a mixture of 1Md and 2M1 illite polytypes. Elevated ratios of the I_{100} and I_{101} quartz diffraction peaks in the oriented preparations indicate the presence of secondary (authigenic) quartz in both Chitwood–Harris and East Fitts samples (Table 1), as also inferred from siliceous cemented intervals in all three cores.

Light and scanning electron microscopy (Fig. 2) reveal sporadic layers <1 cm thick containing algal cysts (Tasmanites). Depending on the sample, Tasmanites are either preserved as OC or completely pyritized (Fig. 2a and b). While readily distinguished, Tasmanites and other visible particulate OC are unlikely to account for a significant fraction of TOC because of their irregular distribution and frequently poor preservation (pyritization).

At the sub-μm scale at which particles comprising the majority of material making up the mudstone intervals can be resolved, TEM micrographs of 80 nm thick ultra-thin sections (Fig. 5) from representative high TOC intervals in the shallowly buried East Fitts core identify micron-scale clay laminae separated by diagenetic quartz, with inclusions of pyrite, dolomite and quartz grains throughout the clay laminae. The sample shows a sharp resin/sample interface with no resin penetration into the sample, the organic carbon within the images is thus not an artefact of the resin impregnation but naturally present in the samples.

The OC identified by EDS within the clay-rich laminae could not be imaged even at the highest magnification (100 nm field of view) and thus must be disseminated within clay aggregates at nanometer or molecular scale. Further, dark-colored homogeneous shapes we initially interpreted as OC 'blebs' similar to those described by

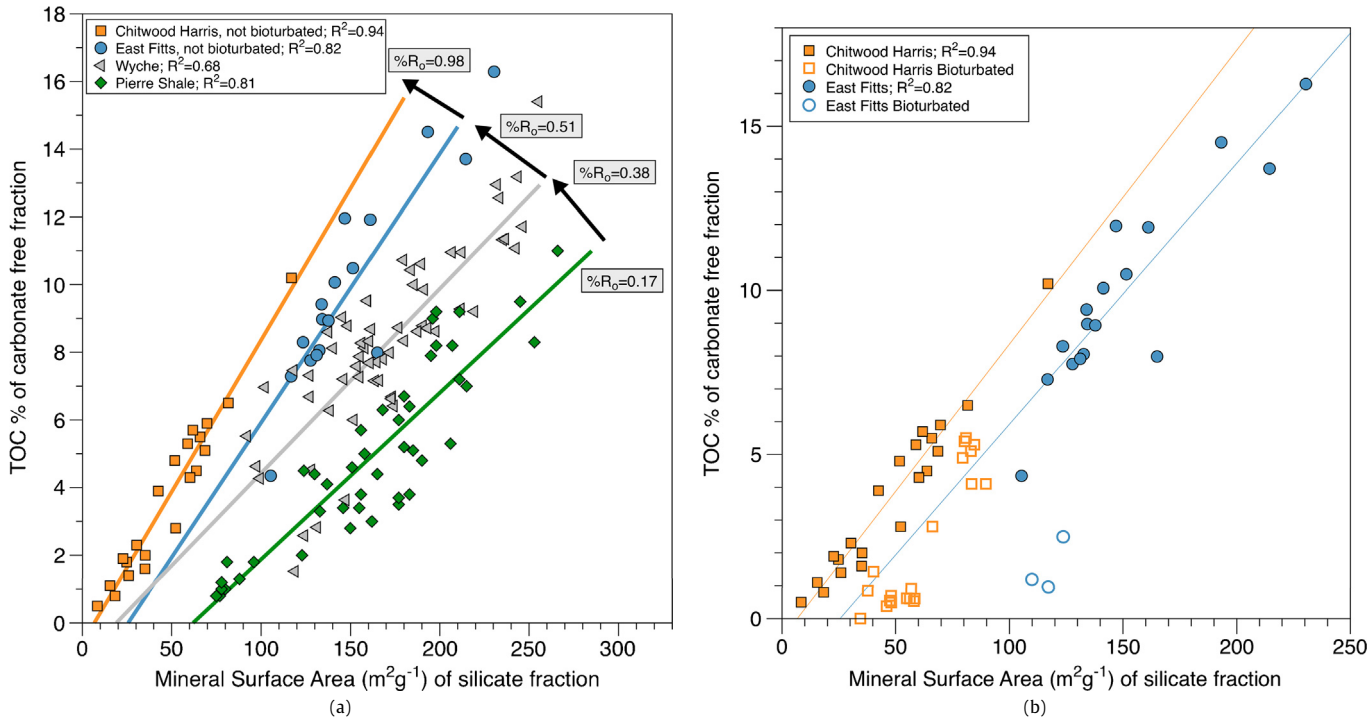

Fig. 3. (a) Silicate MSA plotted against %TOC of the carbonate-free fraction for the Chitwood–Harris (slope = 0.90 mg OC/m^2; %R$_o$ = 0.98), East Fitts (slope = 0.80 mg OC/m^2; %R$_o$ = 0.51) and Wyche (slope = 0.55 mg OC/m^2; %R$_o$ = 0.38) cores, excluding samples from bioturbated intervals for Chitwood–Harris and East Fitts. Samples from the Cretaceous, thermally immature Pierre Shale (from Kennedy et al., 2002) are plotted for comparison (slope = 0.49 mg OC/m^2; %R$_o$ = 0.17). Note that steepening of slope and lower MSA values coincides with increasing thermal maturity from Wyche to East Fitts and to Chitwood–Harris cores, consistent with progressive diagenetic alteration and illitization. (b) Silicate MSA plotted against TOC% of the carbonate-free fraction for the Chitwood–Harris (R^2 = 0.94) and East Fitts (R^2 = 0.82) cores. Samples from bioturbated intervals are plotted separately (open symbols) and are depleted in OC relative to MSA, particularly in heavily bioturbated intervals.

Table 1
Peak ratio indicates authigenic quartz phase values determined by ratios of quartz intensity diffraction peaks I_{100} and I_{101}. Peak ratios confirm the presence of authigenic quartz in all Chitwood–Harris (CH) and East Fitts (EF) samples (values all above the detrital quartz ratio of 0.23 as per Eslinger et al., 1973). Wyche samples were not assessed using this method.

Sample	Intensity		Peak ratio (>0.23 = authigenic quartz)
	Peak 100	Peak 101	
EF-3389.9	120	433	0.28
EF-3414.4	144	496	0.29
EF-3422.4	188	646	0.29
CH-14904.4	241	901	0.27
CH-14916.9	282	775	0.36
CH-14934.9	300	1064	0.28

Salmon et al. (2000) (Fig. 6a) under low magnifications resolved into clay mineral-organic nano-scale composites with increasing magnification (up to 120,000×) (Fig. 6b and c). We identified no discrete, micron-sized particles of OC in the studied ultra-thin sections (Fig. 5).

5. Discussion

The TEM micrographs of the Woodford Shale (Fig. 6) provide the first direct evidence of OC preservation as organo-mineral nanocomposites in ancient OC rich sediments. These images show pervasive interstratification of OC with illite-smectite aggregates and particles at the tens of nanometer scale. EDS analyses confirm that OC is exclusively associated with alumino-silicate regions (Fig. 6), whereas discrete OC not directly associated with clay lamina was not observed.

With the broader field of view possible with standard optical photomicrographs and SEM images, >50 μm-scale particles identified as Tasmanites (Fig. 2a and b) also indicate a range of OC sources in the cores we studied. These different forms of OC record two very different processes of concentration ranging from oceanographic controls of pelagic flux and preservation of organic particles to continental and climatic controls on soil production of high surface area detrital clays supplied from adjacent continental regions. Key to understanding the significance of the carbon concentration of the Woodford Shale is resolving the relative contribution of the different mechanisms of OC preservation. Such identification would result in the separation of dominant mechanisms from other processes that may be evident but do not account for a significant contribution to TOC.

Quantifying the percentage contribution of particulate OC versus nanocomposite associated OC by means of petrographic images has proved to be difficult due to the extreme range of scales at which the different forms of carbon preservation take place. While Tasmanites are evident in some samples, they are usually concentrated in discrete horizons and stratigraphically separated by regions with high TOC but with the form of OC beyond optical resolution. The common practice to deal with this situation is by dissolution of the mineral phase using hydrofluoric acid, thus concentrating the OC that can then be searched for the partial remains of the precursor particles (Taylor et al., 1998). Following this approach, the vast majority (>90%) of OM in Woodford Shale kerogen extracts has no recognizable structure and is classified as 'amorphous' (Lewan, 1983; Senftle, 1989) with the assumption that it represents the fragmentation and diagenetic alteration of Tasmanites particles. The link between Tasmanites-type organic particles and the amorphous, unstructured OM revealed in kerogen separates is only inferred. Alternatively, the amorphous OM fraction may simply be the residue of the organo-mineral nanocomposites after hydrofluoric acid dissolution of the nanocomposite clay mineral host. In either case, the origin of the OC is likely planktonic algae (Tasmanites), be it discrete and recognizable micron-sized particles or nanometer scale compounds broken down by

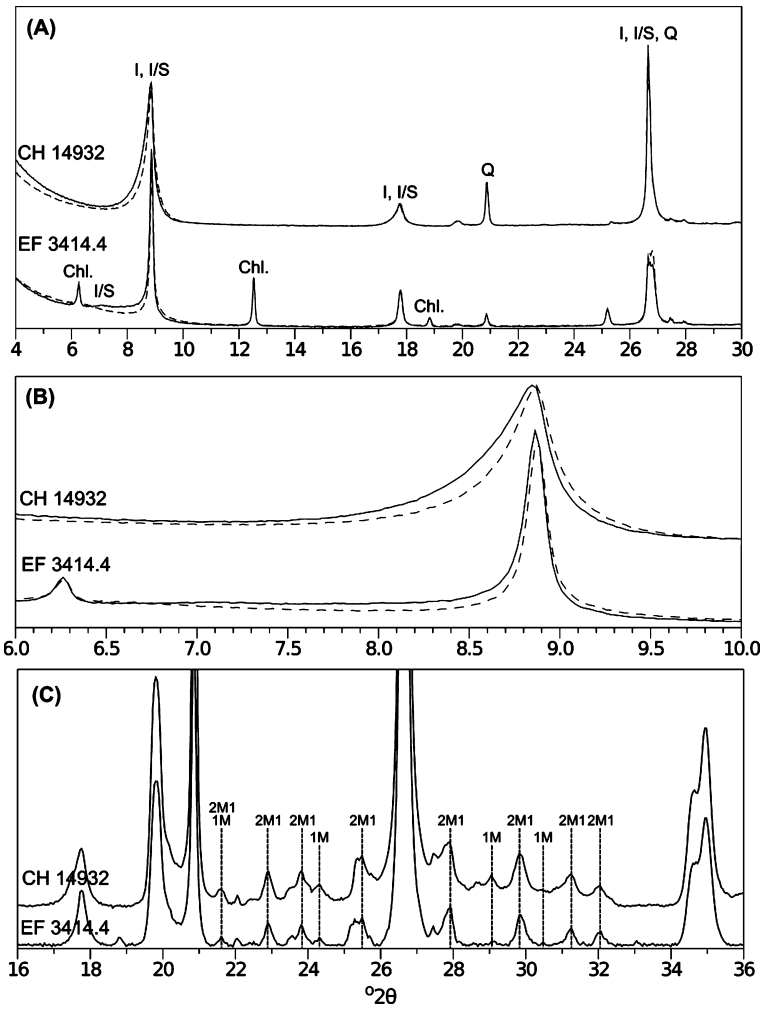

Fig. 4. (A) Representative <2 μm fraction of the clay mineralogy from the Chitwood–Harris core (CH-14932) and East Fitts (EF-3414.4). Air dried (black) and glycolated (dashed grey) diffractograms of oriented preparations showing discrete illite (2M), illite/smectite with <20% smectite interlayers and quartz. The thermally less mature East Fitts samples also contain chlorite. (B) Zoomed in from (A). The high background intensities at $<9^\circ 2\theta$ and the broad, low intensity peak centered at $7.1^\circ 2\theta$ (12.4 Å) are indicative of ordered illite/smectite. Glycolation of the sample results in a drop in intensity of the 8.5 to $6.5^\circ 2\theta$ region, a modest shift of the illite 001 peak to higher angles and increased intensity centered at $26.8^\circ 2\theta$ (3.32 Å), consistent with the presence of R3 ordered, mixed-layer illite/smectite with a smectite component <20% (Eslinger and Pevear, 1988; Reynolds, 1980). (C) XRD pattern of random powder mounts of the <2 μm fraction of typical high TOC (CH) and (EF) samples show that illite is composed of a mixture of 1M and 2M1 illite polytypes, consistent with a mixture of diagenetic (1M) and detrital (2M1) illite.

microbes and diagenetic reactions within the sediment where it became associated with mineral surfaces. In the later case, OC entry into the geologic record is facilitated by the additional step of the physical/chemical interaction with mineral surfaces providing a preservative effect. While clay minerals formed in soils may initially be associated with terrestrial OC, this OC is typically lost with changing ionic composition of river and seawater during transport, with mineral surfaces subsequently becoming associated with marine OC in the water column or (more likely) sediment pores (Keil et al., 1997).

The relative contribution of the clay-organic nanocomposite to the bulk OC is similarly problematic to determine from TEM images alone. While it is possible to identify OC even down to nanometer scales, the limited size of the ultra-thin sections (commonly $<30 \times 30$ μm) and a small field of view means that only a small portion of samples can be imaged, raising the question how representative these views are of the general lithology. To better establish the quantitative role of mineral surfaces on OC preservation as nanocomposites, we link them to the bulk rock property of TOC. We assume that this type of OC preservation maintains a proportionality between TOC and MSA since a mechanistic control of OC preservation by mineral surfaces should result in a reproducible relationship between these two parameters (Mayer, 1994; Hedges and Keil, 1995; Kennedy and Wagner, 2011). As the strength of this relationship declines we assume that other processes control carbon burial, for instance deposition of organic particles that lay outside the narrow field of view of the TEM images.

Throughout the unbioturbated intervals, TOC scales linearly with MSA showing a strong regression in the Chitwood–Harris ($R^2 = 0.94$) and the East Fitts cores ($R^2 = 0.82$) (the Wyche core was not studied for bioturbation, and thus bioturbated samples were not separated). This relationship extends across the full >16% range of TOC values and supports our interpretation that the relationship between mineral surfaces and OC evident in the TEM images is more generally representative of the organic rich intervals in the Woodford Shale. If particulate OC from pelagic sources (and unrelated to mineral surface associated OC) is an important contributor to some portion of the samples that was not imaged, this component would plot above the regression evident in Fig. 3a indicating the presence of OC that was independent and unrelated to the MSA scaling relationship controlled by surface area. No samples are evident in this upper left half of the plot. The hypothesized mechanistic control of carbon preservation by mineral surfaces is further supported by the strong coupling between TOC

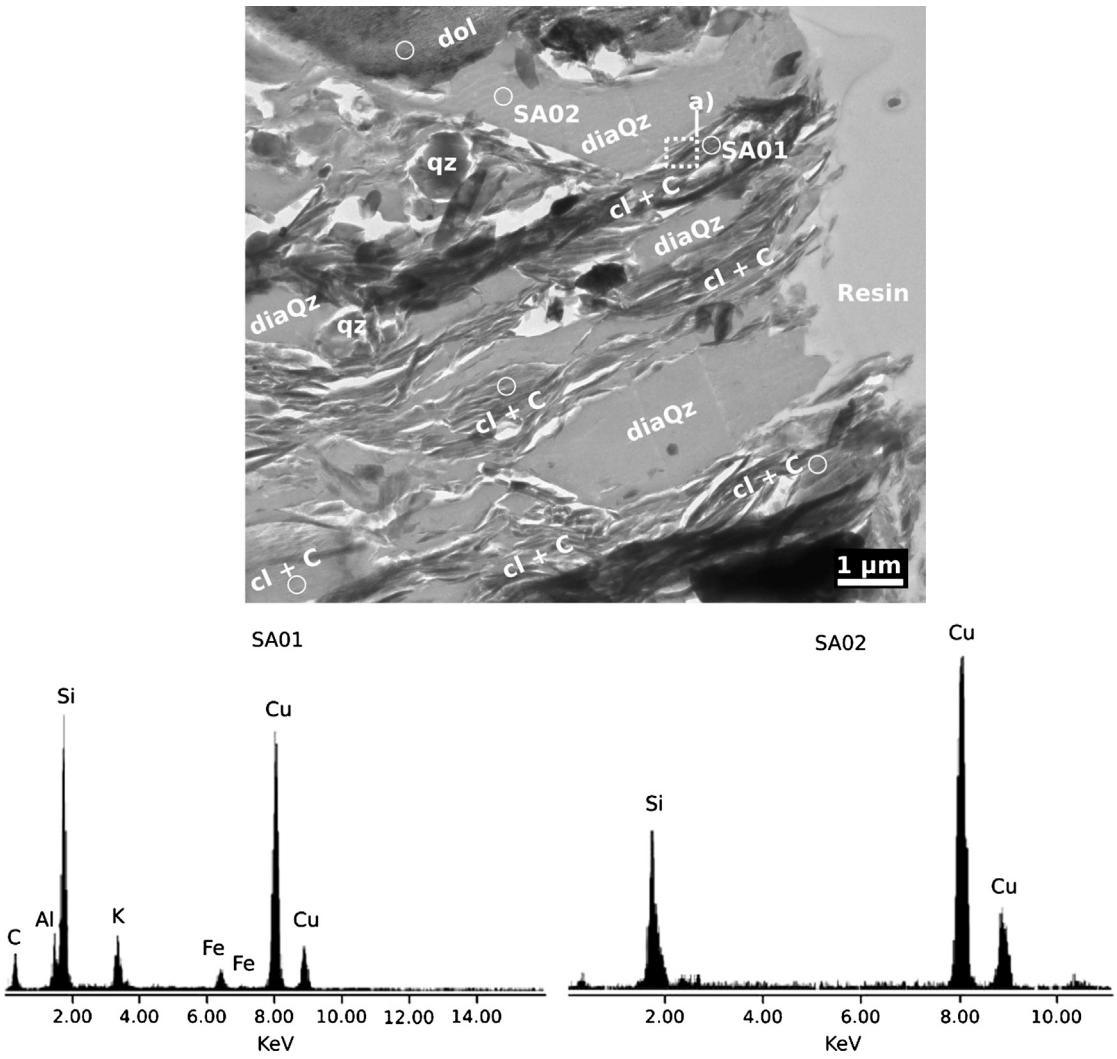

Fig. 5. TEM image of an ultra-thin section from the East Fitts core (sample EF-3422.4). OC is present exclusively within clay layers where it forms a clay-organic nanocomposite (cl + C). There are no exclusive carbon domains. Dolomite is labelled 'dol'. Clay layers are parallel to shale lamination (300–900 nm thick) and are separated by diagenetic quartz labelled 'diaQz'. White circles mark locations of elemental spot analysis by Energy Dispersive Spectroscopy (EDS). Representative spectra at locations SA01 and SA02 are shown and are consistent with clay-organic nanocomposites (SA01) and diagenetic quartz (SA02). Cu peaks are due to Cu sample holder. Dashed square labelled a) marks position of zoomed in micrographs shown in Fig. 6.

and MSA, so that MSA changes in proportion even where there is a >8% jump in TOC from one sample to the next. This contrasts with a lead or lag relation more likely with a shared environmental influence in which changes propagate in a physical record that is slightly out of phase (e.g. Beckmann et al., 2005).

From the consistent relationship between TOC and MSA across the Woodford Shale, we suggest that the organo-mineral nanocomposite evident in Fig. 6 represents the OC classed as the 'amorphous' OC component after the mineral host is dissolved. We further suggest that this component corresponds with the fraction of OC that cannot be separated from the mineral phases by physical fractionation in modern sediment profiles (Keil et al., 1994a; Mayer, 1994) and becomes an increasing proportion of the TOC from the seabed downward, reflecting the physical and chemical breakdown of particulate OC (Keil et al., 1994a). This latter observation leads us to the prediction that further diagenesis with time and burial might yield an increasing proportion of mineral associated OC versus particulate OC in black shales like the Woodford Shale and makes this control of OC preservation more likely in ancient sediments that have passed through the gauntlet of reactions and processes active within the first meter below the seabed.

The relationship between TOC and MSA shows a second order influence where bioturbation is evident (Figs. 1 and 3b). Depth and intensity of burrowing differ through the cores (Fig. 2) suggesting oxygenation or other environmental variability within bottom waters or sediment through time (Kristensen and Kostka, 2005; Schinner, 1993). It is likely that the relatively constant MSA values measured in the upper section of the Chitwood–Harris core (Fig. 1) are the result of biological mixing and homogenization of the sediment. Irrigation resulting in increased oxygenation of the sediment is another consequences of bioturbation (Aller and Aller, 1998; Kristensen and Kostka, 2005). We suggest that the relative depletion of OC in the bioturbated intervals is related to the increased remineralization potential under these conditions (Hartnett et al., 1998; Mackin and Swider, 1989), direct digestion and stripping of OC coatings or the alteration of mineralogy and liberation of interlayer organics in benthic macrofaunal guts (Worden et al., 2006). In any case, the oxygenation of bottom water likely resulted in a reduction of TOC per unit MSA and a greater x-ordinate offset in Fig. 3b indicating OC-free MSA, consistent with other studies (Kennedy and Wagner, 2011; Blair and Aller, 2012). However, retention of some OC and a roughly similar slope in regressions for bioturbated samples suggests a systematic loss of OC from a

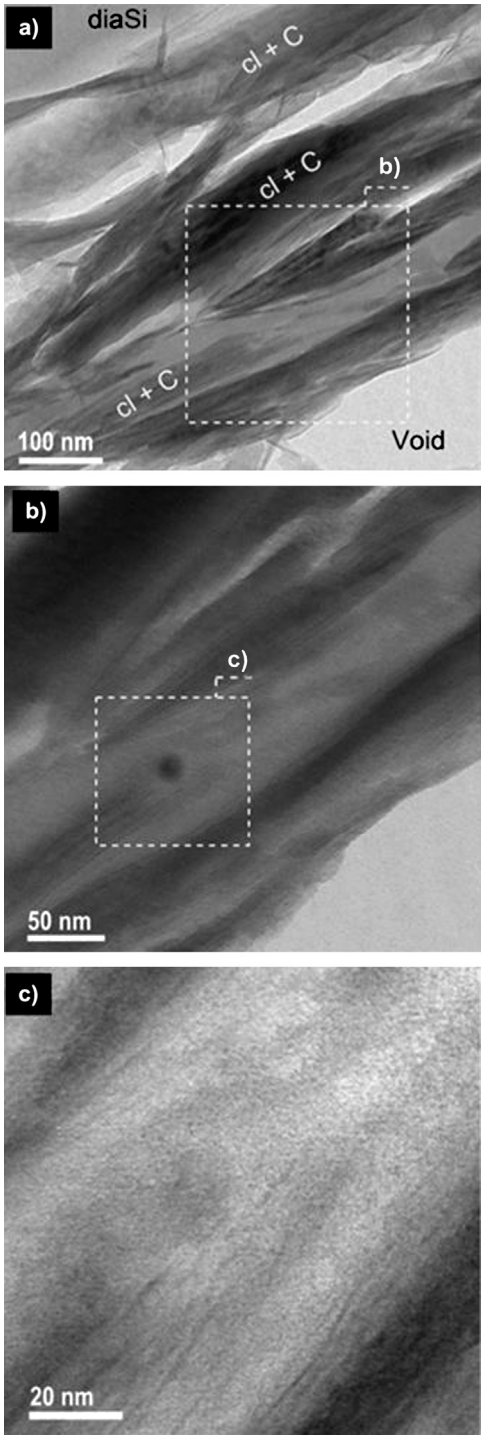

Fig. 6. Zoomed in TEM micrographs of the East Fitts ultra-thin (~80 nm) section shown in Fig. 5. a) corresponds with area marked in Fig. 5 by a box with a dashed line. (a) Clay-organic aggregates (cl + C) enveloping more organic-rich domains up to 90 nm thick. This region is focused on using higher magnification in (b) and (c) and reveal clay particles dispersed within these organic-rich domains indicating that at all scales in this image OC is intercalated with clay minerals as a nanocomposite.

specific component of mineral surfaces, most likely the external surfaces of hydratable clay minerals.

While TOC generally correlates with MSA in modern continental margin sediments, OC loadings per unit MSA are influenced by the depositional environment. Modern loading ratios range from <0.4 mg OC/m^2 for frequently remobilized and re-oxygenated sediments from higher energy settings (e.g. deltaic settings) or deep-sea deposits that are subject to long oxygen exposure times, to 0.4 to 1.0 mg OC/m^2 typical of non-deltaic shelf sediments and >1.0 mg OC/m^2 for sediments from high productivity and/or oxygen-depleted settings (Blair and Aller, 2012). According to this classification, loading ratios (0.55 to 0.90 mg OC/m^2) for non-bioturbated Woodford Shale samples are indicative of non-deltaic shelf sediments rather than the high productivity, low-oxygen environment interpreted on the basis of sedimentological and geochemical evidence. However, MSAs measured using the EGME method in sediments containing smectitic clays are systematically higher compared to the BET method used in the majority of modern sediment studies (see also the discussion in Section 3). Hence, we interpret the relatively low loadings to be the product of high surface areas contributed by residual smectite interlayer surfaces rather than deposition in a typical non-deltaic, shelfal environment.

Although the loading ratios reported here cannot be directly compared with published BET loading ratios, the scaling of the TOC–MSA relationship across 35 to 250 m^2 g^{-1} of MSA and the systematic increases in the loading ratios as a function of thermal maturity provide insights into depositional and burial processes impacting the Woodford Shale. The scaling of TOC:MSA across values of MSA typical of smectite interlayer surface area in other ancient sediments (Kennedy et al., 2002; Kennedy and Wagner, 2011) has led to the hypothesis that the interlayers of smectitic minerals take up both charged and uncharged organic compounds as they do in soils (Theng et al., 1986; Schulten et al., 1996; Baldock and Skjemstad, 2000). This is consistent with mineralogical studies of modern continental margin sediments which show that clays, and the smectite family of minerals in particular, have a close association with OC, starting in the depositional environment (Ransom et al., 1998; Curry et al., 2007). Other clay minerals, even 2:1 minerals like illite, do not have this capacity because the layer charge is too strong to allow expansion and intake of organic compounds to interlayer sites. Such differential preservative capacity is also demonstrated by a recent study which coupled laboratory experiments designed to emulate earliest diagenesis with direct TEM imaging of OM distribution, showing that smectite clays have a markedly stronger preservative effect on OM subjected to enzymatic digestion as compared to illite (Curry et al., 2007).

The Woodford Shale samples considered here, however, represent a marginally mature to mature system with regard to hydrocarbon generation, and have been exposed to conditions that have altered the depositional values of OC and MSA. Measured Woodford Shale MSA values are typically in the range of 35–250 m^2 g^{-1} (Fig. 3), and the clay mineralogy is mostly restricted to the non-expandable clays illite and chlorite, as well as a component of mixed-layer illite-smectite containing $<20\%$ smectite layers. This difference may reflect two possibilities; First, that the MSA–TOC relationship shown in this study was established in the depositional environment by detrital illite surfaces or aggregates interacting with and preserving OM. Or, secondly, that the mixed-layer illite/smectite clay was deposited with a greater proportion of smectite interlayers that were subsequently lost during illitization during burial.

There is, however, strong evidence that the Woodford Shale has undergone typical illitization from an initial depositional mineralogy that included a greater proportion of smectite interlayers. Calculated thermal maturity indicators show that all cores are sufficiently thermally mature for illitization to have commenced. XRD analysis of <2 μm separates shows that the Chitwood–Harris and East Fitts samples contain a mixture of 1Md (diagenetic) and 2M1 (detrital) illite polytypes, whereas analysis of oriented preparations show that the 1Md illite is interstratified with $<20\%$ smectite layers, consistent with partial illitization of smectite or an initially more expandable illite/smectite mixed-layer clay (Pevear, 1999). This is further supported by the abundance of authigenic quartz

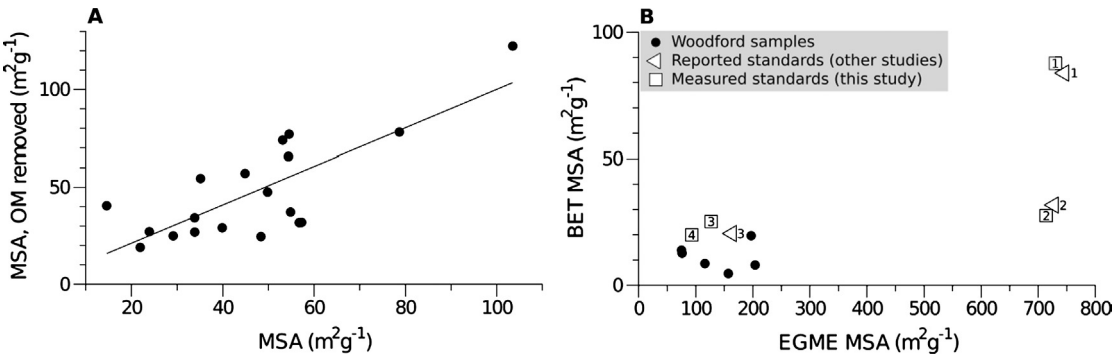

Fig. 7. (A) Comparison of MSA before and after removal of OC with H_2O_2 to determine if there is measurable surface area associated with OC. Samples with the OC removed do not show less MSA indicating that this does not influence the mineral surface determination of MSA. (B) Comparison of EGME and BET surface area values for selected Woodford Shale samples and Clay Mineral Society (CMS) standard clays (numbered squares). Numbered triangles represent reported values for CMS standards. 1 = STx-1b (reported in Środoń and McCarty, 2008); 2 = SWy-2 (Kuila and Prasad, 2011); 3 = IMt-1 (Elzinga and Sparks, 2001); 4 = IMt-2.

in both cores since release of siliceous fluids during smectite illitization commonly results in precipitation of authigenic quartz (Środoń, 1999; Peltonen et al., 2009).

In addition to evidence of thermal maturation and remnant smectite layers within 1Md illite of the Woodford Shale, the palaeogeography of the adjacent Devonian land mass would have favoured smectite production. Smectite is primarily formed in soils subject to warm, seasonally contrasted climates with a distinct dry season and/or settings with limited drainage (Chamley, 1989). It is then eroded and transported to marine environments where it is deposited as a detrital mineral. Palaeogeographic reconstructions of the Late Devonian to Early Mississippian (Scotese, 2012) place the sediment source areas for the Woodford basin in an arid to warm temperate climate zone at a palaeolatitude of 20 to 30°S, comparable to the regions in which smectite is typically formed today.

Comparison to thermally immature ($\%R_o$ = 0.17) smectite and organic rich sediments such as the Cretaceous Pierre Shale (Fig. 3a), also analyzed using the EGME-MSA method and deposited in a high productivity, oxygen-depleted environment similar to that interpreted for the Woodford Shale (Kennedy et al., 2002), can be used to constrain the impact of burial processes on the Woodford Shale. While the Pierre Shale data implies depositional OC loading ratios close to 0.49 mg OC/m^2, the progressively steeper slope evident in each of the Woodford Shale TOC:MSA regressions with $\%R_o$ (thermal maturity) (Fig. 3a), identifies a systematically greater proportion of OC per unit area MSA with increasing thermal maturity, starting with 0.55 mg OC/m^2 for the least thermally mature Wyche core, 0.80 mg OC/m^2 for the East Fitts core and up to 0.90 mg OC/m^2 for the most mature Chitwood–Harris core. The increase in $\%R_o$ corresponds with burial depth in the Wyche, East Fitts and Chitwood–Harris cores, likely reflecting a diagenetic rather than depositional control. To explain this relationship, we propose that the increase in slope of the TOC:MSA regression records the loss of MSA through illitization of smectite layers that initially trapped OC in the depositional and early diagenetic environment in proportion to OC:MSA loading rates similar to those evident in the Pierre Shale (Fig. 3a). Interlayer collapse and surface area reduction associated with illitization expelled and/or polymerized organic compounds in to kerogen (Williams et al., 2005) that was retained in close proximity (sub-micron) with the former host clays (Fig. 6). Thus, illitization resulted in a loss of surface area greater than the loss of generated hydrocarbons, retaining the proportionality between TOC and MSA in these early mature sediments, albeit with a systematically steeper slope.

6. Conclusions

The Woodford Shale is representative of black shale deposits commonly interpreted to result from oceanographic conditions leading to higher marine productivity and/or anoxia (Comer, 1991; Miceli Romero and Philp, 2012). In contrast, our results point to the proportionality of high surface area detrital clay minerals with OC implying the extension of the preservational properties mineral surfaces have in modern sediments. TEM shows direct evidence that this preservation is by organo-mineral nanocomposite association. We argue that organo-mineral nanocomposites account for the majority of TOC in the Woodford Shale based on the strong correlation between MSA and TOC in the three cores analyzed. This relationship would not occur if discrete particles of OC (such as Tasmanites) directly contributed a substantial proportion of OC. The effects on TOC and MSA of bottom-water oxygenation and bioturbation are evident as a modifying effect of this initial relationship. The presence of high surface area detrital clays in the depositional environment, however, was a necessary condition for the greater proportion of OC evident in the Woodford Shale to survive burial from the seabed and enter the geologic record. Systematic loss of MSA through illitization with increasing burial depth and thermal maturity of each core from immature sediments (Pierre Shale) into the oil window (Chitwood–Harris) indicates reorganization of OC, with expulsion from the interlayer sites of smectite and accumulation between illite aggregates. A linear MSA:TOC relationship is retained, however a steepened slope of the MSA:TOC regression identifies the effects of illitization and the reorganization of OC in to clay and organic aggregates.

Given that the vast majority of clay minerals form in soils before being eroded and transported to continental margins, climate and continental processes determine their mineralogy and thus their preservative capacity (e.g. Chamley, 1989). While variable loading rates demonstrate that OC preservation by clay mineral surfaces is not wholly independent of environmental conditions and oceanographic controls such as nutrient availability and bottom-water oxygenation, clay mineral surface preservation of OC suggest that OC enrichments like the Woodford Shale are more closely linked to processes acting on the landward side of continental margin deposits than previously recognized. It also implies that there is a feedback between changing continental climate and carbon burial via the influence of carbon burial efficiency related to clay mineralogy. This mode of carbon burial has significant implications for the mineral composition of unconventional reservoirs and predictions of the distribution of organic carbon rich sediments in basins.

Acknowledgements

We acknowledge Lyn Waterhouse, Dr. Benjamin Wade, Ken Neubauer and Len Green at Adelaide Microscopy for assistance with TEM sample preparation and petrographic analyses. Professor Roger Slatt, Dr. Brian Cardott and the Oklahoma Geological Survey are thanked for providing access to samples. Dr. Tony Hall and Robyn Williamson assisted with laboratory analyses. This work was supported by NSF 09235, ARC LP120200086 and ARC DP110103367.

References

Abid, I., Hesse, R., 2007. Illitizing fluids as precursors of hydrocarbon migration along transfer and boundary faults of the Jeanne d'Arc Basin offshore Newfoundland, Canada. Mar. Pet. Geol. 24, 9.

Ahn, J.H., Cho, M., Buseck, P.R., 1999. Interstratification of carbonaceous material within illite. Am. Mineral. 84, 1967–1970.

Algeo, T.J., Scheckler, S.E., Scott, A.C., 1998. Terrestrial-marine teleconnections in the Devonian: links between the evolution of land plants, weathering processes, and marine anoxic events. Philos. Trans. Biol. Sci. 353, 113–130.

Aller, R.C., Aller, J.Y., 1998. The effect of biogenic irrigation intensity and solute exchange on diagenetic reaction rates in marine sediments. J. Mar. Res. 56, 905–936.

Arthur, M.A., Sageman, B.B., 1994. Marine Black Shales – depositional mechanisms and environments of ancient deposits. Annu. Rev. Earth Planet. Sci. 22, 499–551.

Baldock, J.A., Skjemstad, J.O., 2000. Role of the soil matrix and minerals in protecting natural organic material against biological attack. Org. Geochem. 31, 697–710.

Beckmann, B., Flögel, S., Hofmann, P., Schulz, M., Wagner, T., 2005. Orbital forcing of Cretaceous river discharge in tropical Africa and ocean response. Nature 437, 241–244.

Bergamaschi, B.A., Tsamakis, E., Keil, R.G., Eglington, T.I., Montlucon, D.B., Hedges, J.I., 1997. The effect of grain size and surface area on organic matter, lignin and crarbohydrate concentration and molecular compositions in Peru Margin sediments. Geochim. Cosmochim. Acta 61, 1247–1260.

Blair, N.E., Aller, R.C., 2012. The fate of terrestrial organic carbon in the marine environment. Annu. Rev. Marine Sci. 4, 401–423.

Bock, M., Mayer, L.M., 2000. Mesodensity organo-clay associations in a near-shore sediment. Mar. Geol. 163, 65–75.

Brigatti, M.F., Galan, E., Theng, B.K.G., 2006. Structures and mineralogy of clay minerals. In: Bergaya, F., Theng, B.K.G., Lagaly, G. (Eds.), Handbook of Clay Science. In: Developments in Clay Science, vol. 1. Elsevier, pp. 19–86.

Broadhead, R.F., 2010. The Woodford Shale in southeastern New Mexico: distribution and source rock characteristics. N.M. Geol. 32, 79–90.

Burdige, D.J., 2007. Preservation of organic matter in marine sediments: controls, mechanisms, and an imbalance in sediment organic carbon budgets?. Chem. Rev. 107, 467–485.

Calvert, S., Nielsen, B., Fontugne, M.R., 1992. Evidence from nitrogen isotope ratios for enhanced productivity during formation of eastern Mediterranean sapropels. Nature 359, 223–225.

Chamley, H., 1989. Clay Sedimentology. Springer-Verlag, Berlin.

Chen, G.J., Yen, M.C., Yang, J.M., Lin, J.J., Chiu, H.C., 2008. Layered inorganic/enzyme nanohybrids with selectivity and structural stability upon interacting with biomolecules. Bioconjug. Chem. 19, 138–144.

Comer, J.B., 1991. Stratigraphic Analysis of the Upper Devonian Woodford Formation, Permian Basin, West Texas and Southeastern New Mexico. Report of Investigations, No. 201. Bureau of Economic Geology, Austin.

Curry, K.J., Bennett, R.H., Mayer, L.M., Curry, A., Abril, M., Biesiot, P.M., Hulbert, M.H., 2007. Direct visualization of clay microfabric signatures driving organic matter preservation in fine-grained sediment. Geochim. Cosmochim. Acta 71, 1709–1720.

Dainyak, L.G., Drits, V.A., Zviagina, B.B., Lindgreen, H., 2006. Cation redistribution in the octahedral sheet during diagenesis of illite-smectites from Jurassic and Cambrian oil source rock shales. Am. Mineral. 91, 589–603.

Demaison, G.J., Moore, G.T., 1979. Anozi environments and oil source bed genesis. Org. Geochem. 2, 9–31.

Droser, M.L., Bottjer, D.J., 1993. Trends and patterns of Phanerozoic Ichnofabrics. Annu. Rev. Earth Planet. Sci. 21, 205–225.

Elzinga, E.J., Sparks, D.L., 2001. Reaction conditions on Nickel sorption mechanisms in illite-water suspensions. Soil Sci. Soc. Am. J. 65, 94–101.

Eslinger, E., Pevear, D., 1988. Clay Minerals for Petroleum Geologists and Engineers. SEPM Short Course Notes, vol. 22.

Eslinger, E.V., Mayer, L.M., Durst, T.L., Hower, J., Savin, S.M., 1973. X-ray technique for distinguishing between detrital and secondary quartz in fine-grained fraction of sedimentary-rocks. J. Sediment. Petrol. 43, 540–543.

Hartnett, H., Keil, R.G., Hedges, J., Devol, A., 1998. Influence of oxygen exposure time on organic carbon preservation in continental margin sediments. Nature 391, 572–574.

Hedges, J., Keil, R.G., 1995. Sedimentary organic-matter preservation – an assessment and speculative synthesis. Mar. Chem. 49, 81–115.

Hower, J., Eslinger, E.V., Hower, M.E., Perry, E.A., 1976. Mechanism of burial metamorphism of argillaceous sediment: 1. Mineralogical and chemical evidence. Geol. Soc. Am. Bull. 87, 725–737.

Jarvie, D.M., Claxton, B.L., Henk, F., Breyer, J.T., 2001. Oil and shale gas from the Barnett Shale, Ft. Worth Basin, Texas. In: AAPG National Convention. June 3–6, 2001, Denver, CO, AAPG Bull. 85, A100.

Jia, W., Segal, E., Kornemandel, D., Yamhot, Y., Narkis, M., Siegmann, A., 2002. Polyaniline-DBSA/organophilic clay nanocomposites: synthesis and characterization. Synth. Met. 128, 115–120.

Johnston, C.T., 2010. Probing the nanoscale architecture of clay minerals. Clay Miner. 45, 245–279.

Keil, R.G., Cowie, G.L., 1999. Organic matter preservation through the oxygen-deficient zone of the NE Arabian Sea as discerned by organic carbon: mineral surface area ratios. Mar. Geol. 161, 13–22.

Keil, R.G., Montlucon, D.B., Prahl, F.G., Hedges, J., 1994a. Sorptive preservation of labile organic-matter in marine-sediments. Nature 370, 549–552.

Keil, R.G., Tsamakis, E., Fuh, C.B., Giddings, J.C., Hedges, J., 1994b. Mineralogical and textural controls on the organic composition of coastal marine sediments: Hydrodynamic separation using SPLITT-fractionation. Geochim. Cosmochim. Acta 58, 879–893.

Keil, R.G., Mayer, L.M., Quay, P.D., Richey, J.E., Hedges, J.I., 1997. Loss of organic matter from riverine particles in deltas. Geochim. Cosmochim. Acta 61, 1507–1511.

Kennedy, M.J., Wagner, T., 2011. Clay mineral continental amplifier for marine carbon sequestration in a greenhouse ocean. Proc. Natl. Acad. Sci. USA 108, 9776–9781.

Kennedy, M.J., Pevear, D., Hill, R., 2002. Mineral surface control of organic carbon in black shale. Science 295, 657–660.

Kirkland, D.W., Denison, R.E., Summers, D.M., Gormly, J.R., 1992. Geology and organic geochemistry of the Woodford Shale in the Criner Hills and western Arbuckle Mountains, Oklahoma. In: Johnson, K.S., Cardott, B.J. (Eds.), Source Rocks in the Southern Mid-Continent: 1990 Symposium. Oklahoma Geological Survey Circular, pp. 38–69.

Klemme, H.D., Ulmishek, G.F., 1991. Effective petroleum source rocks of the world – stratigraphic distribution and controlling depositional factors. Am. Assoc. Pet. Geol. Bull. 75, 1809–1851.

Kristensen, E., Kostka, J.E., 2005. Macrofaunal burrows and irrigation in marine sediment: microbiological and biogeochemical interactions. In: Kristensen, E., Haese, R.R., Kostka, J.E. (Eds.), Interactions Between Macro- and Microorganisms in Marine Sediments. American Geophysical Union, Washington, pp. 125–158.

Kuila, U., Prasad, M., 2011. Surface area and pore-size distribution in clays and shales. In: SPE Annual Technical Conference and Exhibition. Denver, Colorado, USA. Society of Petroleum Engineers. SPE 146869, p. 13.

Lewan, M.D., 1983. Effects of thermal maturation on stable organic carbon isotopes as determined by hydrous pyrolysis of Woodford Shale. Geochim. Cosmochim. Acta 47, 1471–1479.

Lindgreen, H., Surlyk, F., 2000. Upper Permian-Lower Cretaceous clay mineralogy of East Greenland: provenance, palaeoclimate and volcanicity. Clay Miner. 35, 791–806.

Lindgreen, H., Drits, V.A., Sakharov, B.A., Salyn, A.L., Wrang, P., Dainyak, L.G., 2000. Illite-smectite structural changes during metamorphism in black Cambrian Alum shales from the Baltic area. Am. Mineral. 85, 1223–1238.

Lo, H.B., Cardott, B.J., 1995. Detection of natural weathering of Upper McAlester coal and Woodford Shale, Oklahoma, U.S.A. Org. Geochem. 22, 73–83.

Mackin, J.E., Swider, K.T., 1989. Organic matter decomposition pathways and oxygen consumption in coastal marine sediments. J. Mar. Res. 47, 681–716.

Mayer, L.M., 1994. Surface-area control of organic-carbon accumulation in continental-shelf sediments. Geochim. Cosmochim. Acta 58, 1271–1284.

Mayer, L.M., 1999. Extent of coverage of mineral surfaces by organic matter in marine sediments. Geochim. Cosmochim. Acta 63, 207–215.

Miceli Romero, A., Philp, R.P., 2012. Organic geochemistry of the Woodford Shale, southeastern Oklahoma: How variable can shales be?. Am. Assoc. Pet. Geol. Bull. 96, 493–517.

Moore, D.M., Reynolds, R.C., 1997. X-ray Diffraction and the Identification and Analysis of Clay Minerals, second ed. Oxford University Press.

Pedersen, T.F., Calvert, S., 1990. Anoxia vs. productivity – what controls the formation of organic-carbon-rich sediments and sedimentary rocks?. Am. Assoc. Pet. Geol. Bull. 74, 454–466.

Peltonen, Marcussen, Bjorlykke, Jahren, 2009. Clay mineral diagenesis and quartz cementation in mudstones: The effects of smectite to illite reaction on rock properties. Mar. Pet. Geol. 26, 12.

Pevear, D.R.D., 1999. Illite and hydrocarbon exploration. Proc. Natl. Acad. Sci. USA 96, 3440–3446.

Ransom, B., Bennett, R., Baerwald, R., Shea, K., 1997. TEM study of in situ organic matter on continental margins: Occurrence and the "monolayer" hypothesis. Mar. Geol. 138, 1–9.

Ransom, B., Kim, D., Kastner, M., Wainwright, S., 1998. Organic matter preservation on continental slopes: Importance of mineralogy and surface area. Geochim. Cosmochim. Acta 62, 1329–1345.

Reynolds, R.C., 1980. Interstratified clay minerals. In: Brindley, G.W., Brown, G. (Eds.), Crystal Structures of Clay Minerals and Their X-Ray Identification. Mineralogical Society, London, pp. 249–300.

Salmon, V., Derenne, S., Lallier-Verges, E., Largeau, C., Beaudoin, B., 2000. Protection of organic matter by mineral matrix in a Cenomanian black shale. Org. Geochem. 31, 463–474.

Satterberg, J., Arnarson, T.S., Lessard, E.J., Keil, R.G., 2003. Sorption of organic matter from four phytoplankton species to montmorillonite, chlorite and kaolinite in seawater. Mar. Chem. 81, 11–18.

Schinner, G.O., 1993. Burrowing Behavior, Substratum Preference, and Distribution of Schizaster canaliferus (Echinoidea: Spatangoida) in the Northern Adriatic Sea. Mar. Ecol. 14, 129–145.

Schulten, H., Leinweber, P., Theng, B.K.G., 1996. Characterization of organic matter in an interlayer clay-organic complex from soil by pyrolysis methylation-mass spectrometry. Geoderma 69, 105–118.

Scotese, C.R. (Ed.), 2012. n.d. PALEOMAP Project. http://www.scotese.com/Default.htm (accessed 12.21.12).

Senftle, J.T., 1989. Influence of kerogen isolation methods on petrographic and bulk chemical composition of Woodford Shale round robin sample. Report of the TSOP Research Committee: The Society for Organic Petrology (TSOP) 6th Annual Meeting, p. 1.

Sherrod, L., Dunn, G., Peterson, G., Kolberg, R., 2002. Inorganic carbon analysis by modified pressure-calcimeter method. Soil Sci. Soc. Am. J. 66, 299–305.

Slatt, R.M., Buckner, N., Abousleiman, Y., Sierra, R., Philp, P., Miceli Romero, A., Portas, R., O'Brien, N.R., Tran, M., Davis, R., Wawrzyniec, T., 2011. Outcrop/behind outcrop (quarry), multiscale characterization of the Woodford Gas Shale, Oklahoma. In: Breyer, J.T. (Ed.), Shale Reservoirs – Giant Resources for the 21st Century. In: AAPG Mem., vol. 97, pp. 1–21.

Sposito, G., Skipper, N.T., Sutton, R., Park, S.H., Soper, A.K., 1999. Surface geochemistry of the clay minerals. Proc. Natl. Acad. Sci. USA 96, 3358–3364.

Środoń, J., 1999. Nature of mixed-layer clays and mechanisms of their formation and alteration. Annu. Rev. Earth Planet. Sci. 27, 19–53.

Środoń, J., McCarty, D.K., 2008. Surface area and layer charge of smectite from CEC and EGME/H_2O-retention measurements. Clays Clay Miner. 56, 155–174.

Taylor, G.H., Teichmüller, M., Davis, A., Diessel, C.F.K., Littke, R., Robert, P., 1998. Organic Petrology. Gebrüder Borntraeger, Berlin.

Theng, B.K.G., Churchman, G.J., Newman, R.H., 1986. The occurrence of interlayer clay-organic complexes in two New Zealand soils. Soil Sci. 142, 262–266.

Tiller, K.G., Smith, L.H., 1990. Limitations of EGME retention to estimate the surface-area of soils. Aust. J. Soil Res. 28, 1–26.

Tyson, R.V., 2001. Sedimentation rate, dilution, preservation and total organic carbon: some results of a modelling study. Org. Geochem. 32, 333–339.

Williams, L.B., Canfield, B., Voglesonger, K.M., Holloway, J.R., 2005. Organic molecules formed in a "primordial womb". Geology 33, 913–916.

Worden, R.H., Needham, S.J., Cuadros, J., 2006. The worm gut; a natural clay mineral factory and a possible cause of diagenetic grain coats in sandstones. J. Geochem. Explor. 89, 428–431.

Zimmerman, A.R., Chorover, J., Goyne, K., Brantley, S.L., 2004. Protection of mesopore-adsorbed organic matter from enzymatic degradation. Environ. Sci. Technol. 38, 4542–4548.